Journal of Crystal Growth 312 (2010) 1311–1315

Contents lists available at ScienceDirect

Journal of Crystal Growth

journal homepage: www.elsevier.com/locate/jcrysgro

Abbreviated MOVPE nucleation of III-nitride light-emitting diodes on nano-patterned sapphire

Yik-Khoon Ee [a,*], Xiao-Hang Li [a], Jeff Biser [b], Wanjun Cao [b], Helen M. Chan [b], Richard P. Vinci [b], Nelson Tansu [a]

[a] Center for Optical Technologies, Department of Electrical and Computer Engineering, Lehigh University, Bethlehem, PA 18015, USA
[b] Center for Advanced Materials and Nanotechnology, Department of Material Science and Engineering, Lehigh University, Bethlehem, PA 18015, USA

A R T I C L E I N F O

Available online 22 October 2009

Keywords:
A1. Nucleation
A1. Substrates
A3. Metalorganic chemical vapor deposition
B1. Nitrides
B2. Semiconducting III–V materials
B3. Light-emitting diodes

A B S T R A C T

Metalorganic vapor phase epitaxy (MOVPE) nucleation studies of GaN on planar sapphire and nano-patterned AGOG (Deposition of **A**luminum, **G**rowth of **O**xide, and **G**rain growth) sapphire substrates were conducted. The use of abbreviated GaN growth mode, which utilizes a process of using 15 nm low-temperature GaN buffer and bypassing etch-back and recovery processes during epitaxy, enables the growth of high-quality GaN template on nano-patterned AGOG sapphire. The GaN template grown on nano-patterned AGOG sapphire by employing abbreviated growth mode has two orders of magnitude lower threading dislocation density than that of conventional GaN template grown on planar sapphire. The use of abbreviated growth mode also leads to significant reduction in cost of the epitaxy. The growths and characteristics of InGaN quantum wells (QWs) light-emitting diodes (LEDs) on both templates were compared. The InGaN QWs LEDs grown on the nano-patterned AGOG sapphire demonstrated a 24% enhancement of output power enhancement over that of LEDs grown on conventional GaN templates.

1. Introduction

A low-dislocation density GaN semiconductor template on sapphire is important for high-efficiency and reliable nitride light-emitting diodes (LEDs) in solid state lighting applications [1 –1 1]. In conventional metalorganic vapor phase epitaxy (MOVPE) of GaN on sapphire substrate, the low-temperature GaN buffer layer is etched-back by employing H_2 at high temperature to form micron-sized GaN islands. The use of intentional delay of the nucleation island coalescence (recovery) reduces threading dislocation density [1]. The etch-back and recovery process employed in conventional MOVPE of GaN on sapphire substrate adds up to 30–45 min to the GaN growth time, which increases the cost of epitaxy process.

The threading dislocation density of conventional MOVPE grown GaN template is still relatively high in the range of 10^8–10^{10} cm^{-2}[2]. Several techniques have been utilized to reduce the threading dislocation density in MOVPE-grown GaN template, such as lateral epitaxial overgrowth (LEO) [3], pendeo epitaxy [4], and cantilever epitaxy [5]. These approaches [3–5] have led to reduction in the dislocation density of GaN template down to 10^6–10^7 cm^{-2}, however the high-quality material was limited to the narrow 2–3 μm stripe regions.

In this work, we studied the MOVPE growths of GaN template on nano-patterned AGOG (Deposition of **A**luminum, **G**rowth of **O**xide, and **G**rain growth) c-plane sapphire substrate by employing abbreviated GaN growth mode (AGGM). Studies of the evolution of the nucleation and growth of GaN using AGGM on nano-patterned AGOG sapphire were performed. The growths of InGaN-based LEDs on both AGGM-based GaN/patterned sapphire and conventional GaN/planar sapphire templates were carried out. The device characteristics of III-Nitride LEDs grown on both templates were compared and analyzed. Cross-sectional transmission electron microscopy (CS-TEM) measurements were performed on both samples. The comparison studies indicated that the use of abbreviated GaN growth mode leads to a two order of magnitude reduction in dislocation densities and improved efficiency in LED devices.

The use of abbreviated GaN growth mode on nano-patterned AGOG sapphire also leads to significant time and epitaxy cost saving, as this process bypasses the conventional etch-back and recovery. By employing the nano-patterned AGOG sapphire, large area (millimeter to wafer size) of high-quality GaN template with lower threading dislocation density can be achieved. The use of high-quality GaN template leads to improved internal quantum efficiency and reliability of LEDs.

* Corresponding author.
E-mail addresses: Ee@Lehigh.Edu (Y.-K. Ee), Tansu@Lehigh.Edu (N. Tansu).

0022-0248/$ - see front matter © 2009 Elsevier B.V. All rights reserved.
doi:10.1016/j.jcrysgro.2009.10.029

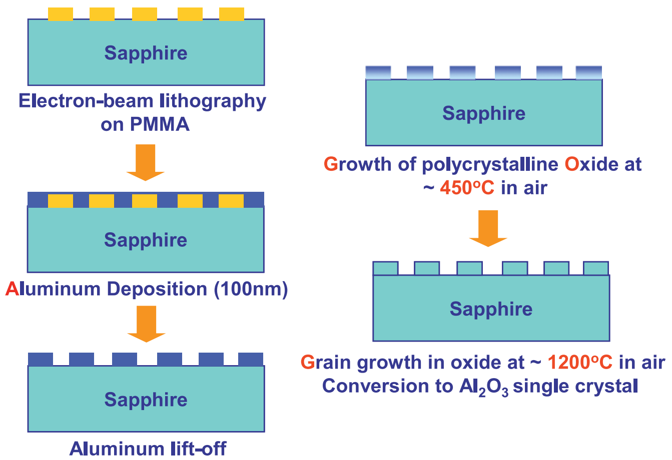

Fig. 1. Schematics of the fabrication process of nano-patterned AGOG sapphire.

2. Nano-patterning of AGOG sapphire substrate

The nano-patterning of sapphire substrate was performed by using a novel AGOG process, which converts metallic aluminum (Al) into single crystal sapphire via a two stage annealing process. The acronym "AGOG" is coined from the process of converting Al into crystalline Al_2O_3 nanostructures [12]: Deposition of **A**luminum, **G**rowth of **O**xide, and **G**rain growth [11,12]. The process schematics of the AGOG sapphire nano-patterning are shown in Fig. 1: (1) Electron-beam patterning of nanostructures on polymethyl methacrylate (PMMA), (2) deposition of 100 nm thick aluminum, (3) aluminum lift-off process leaving behind aluminum nanostructures comprising an array of hexagons approximately 200 nm wide with center-to-center spacing of 400 nm (in our proof-of-concept experiment, the size of the patterned AGOG region was limited to 1 mm × 1 mm), (4) first stage anneal at 450 °C in air to convert metallic aluminum into polycrystalline oxide, and (5) second stage anneal at 1200 °C in air to induce grain growth of the underlying sapphire single crystal to consume the oxide layer. The scanning electron microscopy (SEM) micrographs of the aluminum nanostructures before and after the two annealing stages in the AGOG conversion process are shown in Fig. 2(a) and (b), respectively. As shown in Fig. 2(a) and (b), good shape retention is achieved in the nanostructures after the two annealing processes. To verify that the converted Al nanostructures were crystalline sapphire, electron backscatter diffraction (EBSD) was conducted. Indexing of the patterns confirmed that the patterned AGOG nanostructures consisted of sapphire with the same orientation as the c-plane (0001) substrate [11,12].

3. Abbreviated growth mode on patterned AGOG sapphire

As a control sample, a conventional GaN template was grown on c-plane planar sapphire substrate by employing the conventional method. A 30 nm thick low-temperature (T_g=535 °C) GaN was grown as a buffer layer, followed by the H_2 etch-back and recovery process. The growth of high temperature (T_g=1080 °C) n-GaN (thickness=2.8 μm) was then carried out.

The abbreviated-mode GaN growth was carried out on nano-patterned AGOG sapphire substrate. In this technique, a 15 nm thick low-temperature GaN buffer is grown (T_g=535 °C), followed by the growth of high-temperature GaN *without* the intermediate etch-back and recovery process [11]. The thickness

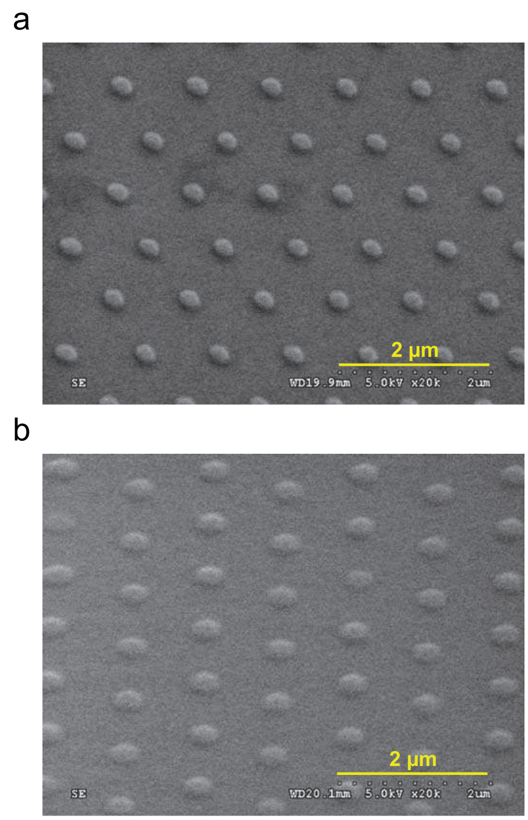

Fig. 2. Scanning electron micrographs of (a) aluminum nano-structure array after lift-off, and (b) aluminum nano-structure array conversion to single crystal Al_2O_3 after two-stage anneal.

of the high-temperature (T_g=1080 °C) n-GaN layer is 2.8 μm. The details of the growth precursors used and the molar flow rate of precursors can be found in reference [11].

To compare the performance of LEDs grown on different GaN templates, the LEDs' active region and p-doped GaN were grown on the conventional GaN template, and the AGOG GaN template in the same epitaxy run. The InGaN-based LED active region consists of four periods of $In_{0.15}Ga_{0.85}N$/GaN (2.5 nm/12 nm) quantum wells (QWs). After the growth of the active region (T_g=740 °C), the growth temperature was ramped up to 970 °C for the growth of p-doped GaN. The n-doping level and p-doping level of GaN were measured as 4.0×10^{18} cm^{-3} and 5.0×10^{17} cm^{-3}, respectively.

4. Nucleation growth experiments

The growth evolution studies of the GaN nucleation on planar and nano-patterned AGOG sapphire substrates were conducted. Fig. 3(a) shows the SEM image of the nano-patterned AGOG region and planar sapphire region after the growth of a 15 nm low-temperature GaN buffer layer (T_g=535 °C). For the case of planar sapphire, the low-temperature GaN nucleated uniformly across the entire region. However, the nucleation process on the nano-patterned AGOG sapphire region is very different from that observed on planar sapphire. Our studies indicated that the low-temperature GaN preferentially nucleates on the patterned region with higher density. From Fig. 3(b), it was clear that the low-temperature GaN preferentially nucleates around the base of the AGOG nano-patterns. The AGOG nano-patterns on sapphire have altered the surface energy, which may cause the low-temperature GaN buffer layer to replicate the nano-patterns

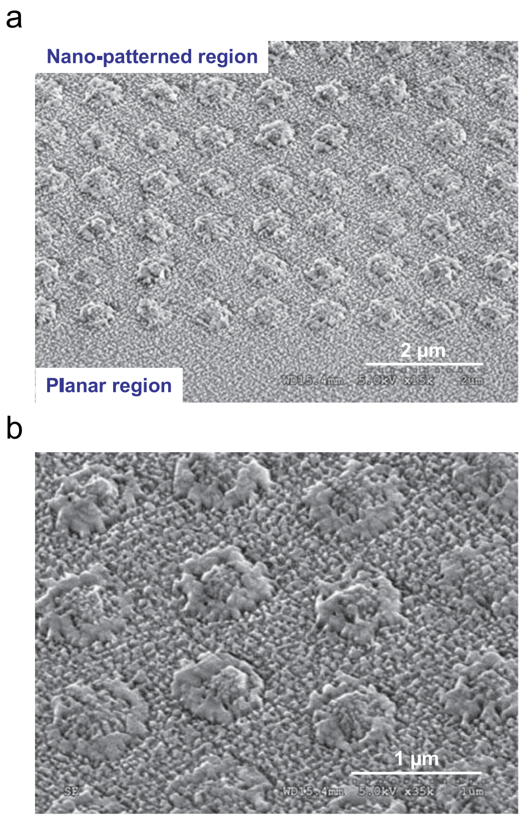

Fig. 3. (a) SEM images of nano-patterned and planar sapphire regions with 15 nm GaN buffer layer, and (b) higher magnification SEM image of the nano-patterned sapphire region with 15 nm GaN buffer layer.

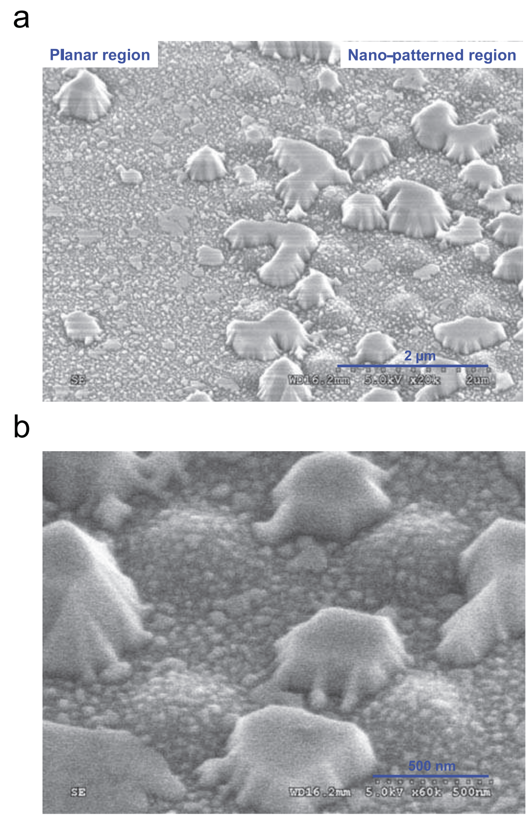

Fig. 4. (a) SEM images of nano-patterned and planar sapphire regions with 15 nm GaN buffer layer and 3 min growth of high-temperature GaN, and (b) higher magnification SEM image of the nano-patterned sapphire with 15 nm GaN buffer layer and 3 min growth of high-temperature GaN.

by preferentially growing surrounding the existing AGOG nano-patterns.

After 3 min of high-temperature (T_g=1080 °C) GaN growth via abbreviated GaN growth mode, the GaN growth was interrupted. The SEM image of the GaN material grown on the nano-patterned AGOG region and planar sapphire region is shown in Fig. 4(a). As shown in Fig. 4(a), high-temperature GaN islands prefentially grow on the patterned AGOG sapphire due to the higher density of the low-temperature GaN nuclei on the nano-patterned AGOG region. Thus, this result in higher density of high-temperature GaN islands grown on the nano-patterned AGOG region. As shown in Fig. 4(b), our studies indicated that larger single crystal high-temperature GaN islands preferentially grow in the valley region of the AGOG nano-patterns during the initial growth stage. The growth of high-temperature GaN starts from the low-temperature GaN islands, hence this implies that the low-temperature GaN in the AGOG nano-patterened region could have re-arranged its position from surrounding the AGOG nano-patterns to the regions between nano-patterns during the high-temperature ramp up for the GaN growth. The re-arrangement of low-temperature GaN during high-temperature ramp up was also observed in high-temperature TEM experiments done by Amano and Akasaki [13].

Previous works have indicated that the threading dislocations bent when micron-sized GaN island coalesced [14]. Note that the nano-scale GaN islands formed in the initial growth of high-temperature GaN on patterned sapphire [Fig. 4(b)] preferentially nucleate on the nano-patterned AGOG region, thereby providing more GaN islands for coalescence. The increased interfaces for GaN island coalescence enhance the probability for the threading dislocations to bend, improving the GaN material quality.

The growths of 0.1μm thick [Fig. 5(a)] and 0.25μm thick [Fig. 5(b)] high-temperature GaN (by abbreviated growth mode) were conducted on nano-patterned AGOG and planar sapphire samples. The surface morphologies of the GaN material grown on these two regions were very different. In Fig. 5(a), the preferential growth of high-temperature GaN on nano-patterned AGOG region was evident as the GaN has started to coalesce at a much earlier stage, as compared to the coalescence for GaN grown on the planar sapphire. From Fig. 5(b), we observe that at 0.25 μm the high-temperature GaN has completely coalesced forming a smooth film on the nano-patterned sapphire, but not on the planar region. The use of the abbreviated growth mode on nano-patterned sapphire provides significant advantage over the conventional approach, as this approach leads to significant cost reduction and epitaxy time.

5. LED characteristics and TEM results

Fig. 6 shows the light output power as a function of injection current for the 445 nm emitting InGaN QWs LEDs grown on different GaN templates as follows: GaN template grown by abbreviated growth mode on nano-patterned AGOG sapphire (LED-1), GaN template grown by conventional technique on planar sapphire (LED-2), and GaN template grown by abbreviated growth mode on planar sapphire (LED-3). The LED devices with areas of 1.25 $\times$ 10^{-3} cm^2 were measured under continuous wave (CW) condition at room temperature. The output power and efficiency of LED-1 (employing AGGM growth on patterned sapphire) exhibited a 24% enhancement in comparison to those of the conventional LED-2. As for the LED-3 (without the etch-back and recovery process during the GaN template growth

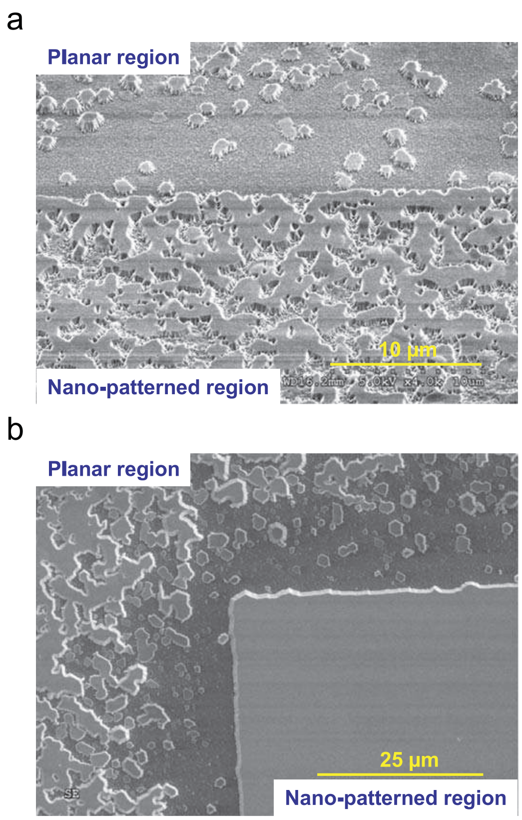

Fig. 5. SEM images of (a) nano-patterned and planar sapphire regions with 15 nm GaN buffer layer and 0.1 µm thick high-temperature GaN, and (b) nano-patterned and planar sapphire regions with 15 nm GaN buffer layer and 0.25 µm thick high-temperature GaN.

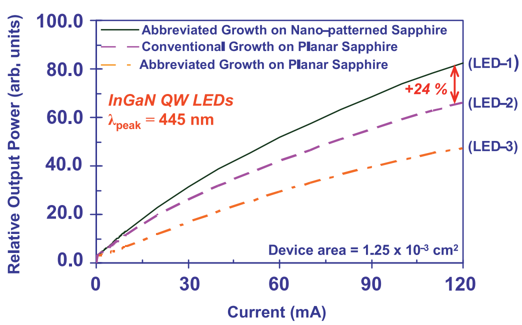

Fig. 6. Room temperature CW light output power as a function of injection current of $In_{0.15}Ga_{0.85}N$ QW LEDs grown on three comparison templates (LEDs #1, #2, and #3).

on planar sapphire), its output power was measured as 28% lower than that of the conventional LED-2.

The cross-sectional TEM micrographs of the LED samples grown on nano-patterned AGOG substrate with abbreviated growth mode (LED-1) and conventional GaN template (LED-2) are shown in Fig. 7(a) and (b), respectively. Preliminary measurements indicate that the threading dislocation density of the GaN grown on nano-patterned AGOG sapphire and GaN grown on planar sapphire were 3×10^{7} cm^{-2} and 1×10^{9} cm^{-2}, respectively. Using nano-patterned AGOG sapphire and abbreviated GaN growth mode, the threading dislocation density was approximately two orders of magnitude lower than on a conventional GaN template. The improvement observed in the output power of LED-1 can be attributed to the enhanced radiative efficiency of the InGaN QWs LEDs, due to a reduction in threading

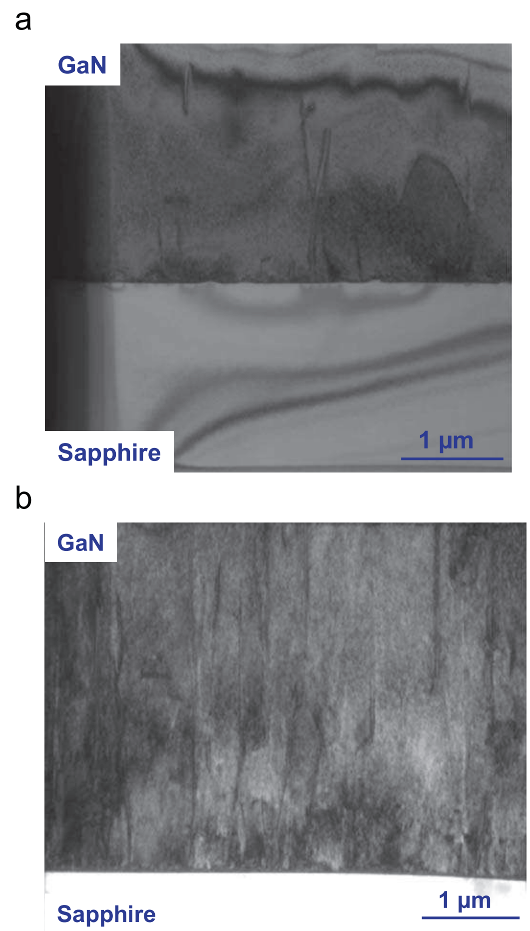

Fig. 7. Cross-sectional TEM images taken at g=(0002) for (a) LEDs sample grown on nano-patterned sapphire with abbreviated growth mode, and (b) LED sample grown on planar sapphire using conventional growth.

dislocation density in the GaN template grown on nano-patterned AGOG sapphire substrate.

The proof-of-concept experiments show that the GaN abbreviated growth mode on nano-patterned AGOG sapphire substrate leads to reduction in the threading dislocation density in the GaN template. The use of GaN abbreviated growth mode also reduces epitaxy time and cost. Although electron-beam patterning of the substrate is impractical as a production tool, other large-scale and low-cost lithography processes such as holography or sol–gel lithography approaches can be used to nano-pattern large batches of substrates. Once the large scale nano-patterning can be implemented, the thermal processing of the substrates can be performed as a batch process at relatively low cost.

6. Summary

In conclusion, nano-patterning of the sapphire substrate was conducted by using a novel AGOG process. By employing the nano-patterned AGOG sapphire, the use of GaN abbreviated growth mode could be conducted thereby reducing epitaxy cost and time. The abbreviated growth mode comprises a thin 15 nm low-temperature GaN buffer, followed by high-temperature GaN growth without the etch-back and recovery process. Studies of the abbreviated growth mode nucleation and growth of GaN were carried out. Our studies indicated that low-temperature GaN buffer layers were preferentially nucleating on the nano-patterned AGOG region, and the growth of high-temperature

GaN also showed preferential coalescence at a much earlier stage compared to the high-temperature GaN in the planar sapphire region.

Comparison studies were also conducted on 445 nm emitting InGaN QWs LEDs grown on both patterned and planar sapphire substrates. The LEDs grown on the GaN template on nano-patterned AGOG sapphire with GaN abbreviated growth mode demonstrated 24% improvement in the output power over the LEDs grown on conventional GaN template. The improvement observed in the LEDs grown on patterned sapphire substrates can be attributed to the two orders of magnitude reduction in the threading dislocation density observed from the TEM measurements. The use of abbreviated growth mode enables the epitaxy of low-dislocation density GaN on patterned AGOG sapphire substrate, without the need of etch-back and recovery process.

Acknowledgements

The authors would like to acknowledge funding support from the US Department of Energy (DE-FC26-08NT01581) and US National Science Foundation (ECCS # 0701421, and DMR # 0705299).

References

1 D.D. Koleske, A.J. Fischer, A.A. Allerman, C.C. Mitchell, K.C. Cross, S.R. Kurtz, J.J. Figiel, K.W. Fullmer, W.G. Breiland, Appl. Phys. Lett. 81 (2002) 1940–1942.
2 S. Nakamura, Science 281 (1998) 956–961.
3 M. Hansen, P. Fini, M. Craven, B. Heying, J.S. Speck, S.P. DenBaars, J. Cryst. Growth 234 (2002) 623–630.
4 A.M. Roskowski, E.A. Preble, S. Einfeldt, P.M. Miraglia, R.F. Davis, IEEE J. Quantum Electron. 38 (2002) 1006–1016.
5 C.I.H. Ashby, C.C. Mitchell, J. Han, N.A. Missert, P.P. Provencio, D.M. Follstaedt, G.M. Peake, L. Griego, Appl. Phys. Lett. 77 (2000) 3233–3235.
6 R.A. Arif, Y.K. Ee, N. Tansu, Appl. Phys. Lett. 91 (2007) 091110.
7 Y.K. Ee, P. Kumnorkaew, R.A. Arif, J.F. Gilchrist, N. Tansu, Appl. Phys. Lett. 91 (2007) 221107.
8 Y.K. Ee, P. Kumnorkaew, R.A. Arif, H. Tong, H. Zhao, J.F. Gilchrist, N. Tansu, IEEE J. Sel. Top. Quantum Electron. 15 (2009) 1218–1225.
9 H. Zhao, G.S. Huang, G. Liu, X.H. Li, J.D. Poplawsky, S. Tafon Penn, V. Dierolf, N. Tansu, Appl. Phys. Lett. 95 (2009) 061104.
10 H. Zhao, R.A. Arif, N. Tansu, IEEE J. Sel. Top. Quantum Electron. 15 (2009) 1104–1114.
11 Y.K. Ee, J.M. Biser, W. Cao, H.M. Chan, R.P. Vinci, N. Tansu, IEEE J. Sel. Top. Quantum Electron. 15 (2009) 1066–1072.
12 H. Park, H.M. Chan, R.P. Vinci, J. Mater. Res. 20 (2004) 417–423.
13 H. Amano, I. Akasaki, J. Phys. Condens. Matter 13 (2001) 6935–6944.
14 K. Hiramatsu, K. Nishiyama, M. Onishi, H. Mizutani, M. Narukawa, A. Motogaito, H. Miyake, Y. Iyechika, T. Maeda, J. Cryst. Growth 221 (2000) 316.